EVALUATION OF IMPROVED SPATIAL AND SPECTRAL RESOLUTION ON MODEL BASED FITTING OF PROSTATE SPECTROSCOPY AT 7 TESLA

Gregory J. Metzger[1], Edward Auerbach[1], Christopher A. Warlick[2], Diane Hutter[1], Gregory Adriany[1], and Ivan Tkac[1]
[1]*Center for Magnetic Resonance Research, University of Minnesota, Minneapolis, MN, United States,* [2]*Department of Urologic Surgery, University of Minnesota*

INTRODUCTION: As demonstrated in the brain, the advantage of performing spectroscopy at higher magnetic fields is the improved quantification of metabolites due to increased spectral dispersion and signal to noise ratio (SNR) (1). While prostate spectroscopy at higher magnetic fields is expected to realize a similar advantage, the impact on the quantification of prostate specific metabolites observed in vivo needed to be investigated. An initial evaluation of this impact is made in this work through simulations and quantification of in vivo data at field strengths of 3T and 7T. It will be demonstrated that improved delineation between overlapping metabolites is possible at higher fields as indicated by improved Cramer-Rao lower bounds (CRLB) and reduced correlation coefficients (CC) between peaks.

METHODS: *Simulations:* Simulations were performed for spectra with varying relative levels of prostate metabolites representing "normal", "probably-cancer" and "definitely cancer" spectral patterns. Individual peaks were generated by solving the Liouville equation and making use of each metabolite's chemical shift and *J*-coupling information (2). Metabolites of interest included choline containing compounds (glycerophosphocholine (GPC), phosphocholine (PCho) and choline (Cho)), spermine (Spm) which represents the polyamine signal, creatine (Cre) and citrate (Cit). For spermine, the couplings and chemical shifts were previously estimated from sample solutions run at 600 MHz (3). To simplify the simulation and the interpretation of results, an excite-acquire experiment was assumed. After combining the different resonances, noise was added to approximate a 50% higher spatial resolution and 50% higher SNR for 7T as compared to 3T. Therefore, the theoretical increase in SNR was split between higher spatial resolution and improved signal intensity as might be done in practice. To account for the expected increase in line broadening due to field strength dependent susceptibility effects, 7T linewidths were increased 50% to 12 Hz compared to 3T (8Hz). The original metabolite signals used to generate the final spectra constituted the basis set used for fitting the simulated data.

In vivo LCModel Fitting: LCModel, a frequency domain fitting method initially developed for processing brain spectroscopy, has also been shown to be useful in processing 3T, 3DSI prostate data (3,4,5). The basis functions used for LCModel fitting were generated by solving the Liouville equation accounting for the specific RF pulses and timing details of the field dependent acquisition sequence for all metabolites except spermine. The chemical shift and coupling estimates previously made for spermine were not adequate to simulate the evolution of spermine's 20 protons over the 145 ms echo times used for the in vivo acquisitions. Therefore, for spermine, a basis function was directly measured experi mentally by acquiring data with the acquisition parameters of the in vivo 3DSI sequences.

In vivo 3D Spectroscopic Imaging (3DSI): Healthy subjects were imaged at both 3T and 7T under an IRB approved protocol. Anatomic scout T2w turbo spin echo (TSE) images were acquired for planning purposes. Studies at both 3T and 7T used an endorectal (ERC) combined surface array for signal reception with the ERC filled with perfluorocarbon to reduce susceptibility effects. For transmit, the 3T study used the standard clinical system's body coil which is on the outside of the bore liner while at 7T, a 16 channel surface array was used for transmit. The complete 7T RF coil configuration, RF management and safety evaluation has been previously reported (7). At 3T, PRESS was used for localization with sequence timing following that detailed by Scheenen et al. (8). Sequence parameters included: TR/TE 750/145 ms, 12x12x8 acquisition matrix, 2000 Hz bandwidth, 8 weighted averages and a nominal voxel resolution of 180 µL. At 7T, localization was achieved by using semi-LASER (9). Sequence parameters included: TR/TE 2000/145 ms, 16x16x8 acquisition matrix, 4 kHz bandwidth, 4 weighted averages and nominal voxel resolution of 80 µL. VAPOR water suppression (10) and dual banded MEGAwere also used (11).

RESULTS / DISCUSSION: *Simulations:* The CRLB for the simulated metabolites in for the various metabolite profiles are shown in Figure 1. As GPC and PC are indistinguishable at both field strengths these peaks are combined. The 3T data always have higher CRLB, corresponding to lower confidence in the fitted peak amplitudes, than the 7T data except for the citrate peak in the "definitely cancer" spectrum where the choline signal is much higher than citrate. *In Vivo:* A single representative spectrum obtained from a voxel at the same spatial location from 3DSI data sets obtained 3T and 7T in are shown in Figures 2 and 3, respectively. The black curves represent the acquired data and the red curves the individual fitted contributions from metabolites in the basis set. The 7T data presents with lower SNR due to several factors including: 1) lower voxel volumes (80 µL at 7T and 180 µL at 3T), 2) expectation of appreciably shorter T2s at 7T and the use of the same long echo time of 145 ms at both field strengths 3) differences in spatially varying receive profiles and 4) differences in coil performance. Despite this lower SNR, the in vivo 7T data show better fitting accuracy with decreased CRLB and lower CC as shown in the two tables, indicating that even with the current acquisition parameters, improved quantification accuracy can be achieved with more than twice the spatial resolution. The in vivo CRLB and CC were evaluated in all spectra within the prostate from a single slice (i.e. 35 voxels). Consistently lower CRLB and CC, as demonstrated by the low standard deviations, demonstrate that quantification is better across the entire depth of prostate.

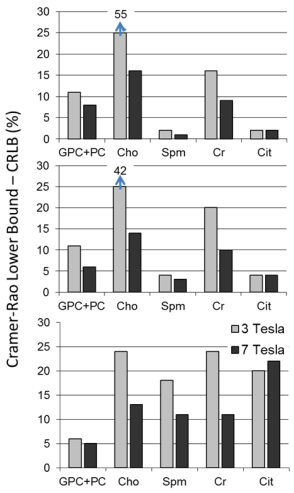

Figure 1: Simulation: CRLB for the normal (top), probably-cancer (middle), and definitely cancer (bottom) profiles.

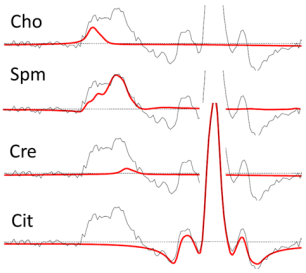

Figure 2: In vivo 3T 3DSI LCModel fit from a selected voxel. (180 µL)

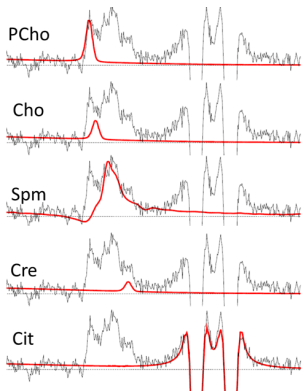

Figure 3: In vivo 7T 3DSI LCModel fit from the same spatial location as in Fig. 2. (80 µL).

CRAMER-RAO LOWER BOUND - CRLB (%)				
		3T	*7T*	*7T / 3T*
SIMULATION	*Total Cho*	14	6	0.43
(Normal Profile)	*Spermine*	8	4	0.50
	Creatine	69	27	0.39
	Citrate	2	2	1.00
IN VIVO	*Total Cho*	11 ± 3	8 ± 2	0.73
(35 voxel $\mu \pm \sigma$)	*Spermine*	9 ± 3	4 ± 1	0.44
	Creatine	n/a	31 ± 7	n/a
	Citrate	4 ± 2	2 ± 1	0.50

CORRELATION COEFFICIENTS (CC) WITH SPERMINE				
		3T	*7T*	*7T / 3T*
SIMULATION	*Total Cho*	-0.44	-0.12	0.27
(normal profile)	*Creatine*	-0.39	-0.18	0.46
IN VIVO	*Total Cho*	0.55 ± 0.19	0.12 ± 0.15	0.22
(35 voxel $\mu \pm \sigma$)	*Creatine*	-0.36 ± 0.12	-0.20 ± 0.15	0.56

These results indicate that there are more important factors for accurate quantification beyond SNR. The increased spectral dispersion, especially for choline and creatine which overlap with the strongly coupled spermine signal, greatly benefit from quantification at increased field strength. The ability to individually quantify these metabolites may prove clinically relevant. For example, HRMAS data from Swanson et al. demonstrate that the polyamine resonance was most correlated with cancer aggressiveness (12). While the results presented will be different depending on the exact acquisition methods employed and the timing parameters used, this work demonstrates that improved fitting based on lower CRLB and CC exist over a wide range of metabolite profiles and conditions from a simulated FID to data acquired in vivo at an echo time of 145 ms.

REFERENCES: [1] Tkac, MRM 2009;62(4):868. [2] Henry, MRM 2006;55(2):250. [3] Metzger, ISMRM, 2007:802. [4] McLean, MRM 2011; 65(4):914. [5] Garcia-Martin, MRM 2011;65(2):329. [6] Metzger, MRM 2010;64(6):1625. [7] Scheenen, MRM 2005;53(6):1268. [8] Scheenen, Magma 2008;21(1-2):95. [9] Tkac, MRM 1999;41(4):649. [10] Mescher, NMR Biomed 1998;11(6):266. [11] Metzger, MRM 2010; 64:1625. [12] Swanson, MRM 2003;50(5):944.

ACKNOWLEDGEMENTS: Funding Provided by R01 R01CA131013, R01 R01CA131013-S1, BTRC P41 RR008079 and the Keck Foundation S10 RR026783.